MYC Can Induce DNA Breaks *In vivo* and *In vitro* Independent of Reactive Oxygen Species

Suma Ray,[1] Kondala R. Atkuri,[2] Debabrita Deb-Basu,[1] Adam S. Adler,[3] Howard Y. Chang,[3] Leonore A. Herzenberg,[2] and Dean W. Felsher[1]

[1]Division of Oncology, Departments of Medicine and Pathology, [2]Genetics, and [3]Dermatology, Stanford University School of Medicine, Stanford, California

Abstract

MYC overexpression is thought to initiate tumorigenesis by inducing cellular proliferation and growth and to be restrained from causing tumorigenesis by inducing cell cycle arrest, cellular senescence, and/or apoptosis. Here we show that MYC can induce DNA breaks both *in vitro* and *in vivo* independent of increased production of reactive oxygen species (ROS). We provide an insight into the specific circumstances under which MYC generates ROS *in vitro* and propose a possible mechanism. We found that MYC induces DNA double-strand breaks (DSBs) independent of ROS production in murine lymphocytes *in vivo* as well as in normal human foreskin fibroblasts (NHFs) *in vitro* in normal (10%) serum, as measured by γH2AX staining. However, NHFs cultured *in vitro* in low serum (0.05%) and/or ambient oxygen saturation resulted in ROS-associated oxidative damage and DNA single-strand breaks (SSBs), as measured by Ape-1 staining. In NHFs cultured in low versus normal serum, *MYC* induced increased expression of *CYP2C9*, a gene product well known to be associated with ROS production. Specific inhibition of *CYP2C9* by small interfering RNA was shown to partially inhibit *MYC*-induced ROS production. Hence, MYC overexpression can induce ROS and SSBs under some conditions, but generally induces widespread DSBs *in vivo* and *in vitro* independent of ROS production. (Cancer Res 2006; 66(13): 6598-605)

Introduction

The *MYC* proto-oncogene encodes a transcription factor of which the activity has been implicated in diverse functions including cellular growth and proliferation, differentiation, angiogenesis, cellular adhesion, and apoptosis (1). Overexpression of *MYC* is thought contribute to tumorigenesis by enforcing unrestrained cellular growth and proliferation (1, 2). *MYC* and other oncogenes may also contribute to tumorigenesis through the induction of genomic destabilization (3–14). *MYC*-induced DNA damage may account for the observed proliferative arrest, senescence, and apoptosis of normal human foreskin fibroblasts (NHF) or mouse embryonic fibroblasts *in vitro* (9, 15). Several studies have suggested that *MYC* may induce genomic damage *in vivo* (6, 16, 17).

MYC overexpression is associated with abnormalities in chromosomal number, chromosomal breaks, and translocations (7). *MYC* has been proposed to induce chromosomal damage through at least three possible non-mutually exclusive mechanisms. First, *MYC* may enforce cell cycle transit abrogating mechanisms that preserve genomic integrity or mediate DNA repair by interfering with the repair of DNA double-strand breaks (DSBs; refs. 7, 12, 18). Second, *MYC* and other oncogenes may cause DNA breaks through the induction of reactive oxygen species (ROS; refs. 19–23). Third, *MYC* has been shown to result in breakage-bridge-fusion cycles and telomere remodeling (24). The relative contribution of these different mechanisms is not known.

Many studies document that ROS can lead to genomic instability and contribute to tumorigenesis (19, 25). ROS can directly result in DNA single-strand breaks (SSBs) or DSBs; purine, pyrimidine, or deoxyribose modifications; and DNA cross-links (26, 27). ROS can be produced from both exogenous and endogenous sources. One such potential endogenous source of ROS is cytochrome *P*450 (*CYP450*) metabolism. The various mechanisms that regulate production of ROS by *CYP450* in different cells and tissues have been widely discussed (28, 29).

To evaluate if *MYC* can induce DNA breaks in normal cells under physiologic circumstances and if these breaks are mediated by the production of ROS, we have examined the consequences of conditional *MYC* activation *in vitro* in NHFs and *in vivo* in normal murine lymphocytes using the Tet System (30). We found that MYC overexpression can induce DNA breaks *in vivo* and *in vitro* in normal cells through mechanisms independent of ROS production.

Materials and Methods

Cell culture. NHFs were grown in DMEM without phenol red and supplemented with 10% fetal bovine serum (FBS) and penicillin/streptomycin. In some experiments, cells were grown *in vitro* in media containing low serum (0.05% FBS) for 48 hours before *MYC* induction. Fibroblasts were infected with pBabe-puro retrovirus containing *MYCER* (7, 31).

Induction of *MYC* activity. *MYC* was induced in NHFs with *MYCER* (NHF-*MYCER*) using 4-hydroxy tamoxifen (4-OHT; Sigma-Aldrich, St. Louis, MO), added to the medium at a final concentration of 1 μmol/L.

Transgenic mice. For *in vivo* studies, we used a transgenic mouse line with the tTA System in which *MYC* is conditionally expressed in T cells with the help of a tissue-specific promoter (30).

Confocal microscopy for detection of ROS in *MYC*-induced NHFs. To investigate the production of ROS in *MYC*-induced NHFs, NHF-*MYCER* cells were grown on coverslips in 24-well tissue culture dishes in normal and low serum and *MYC* was induced for 4 hours with 4-OHT. Cells were treated with 1 μmol/L of an antioxidant, *N*-acetyl cysteine (NAC; Sigma-Aldrich), overnight, before *MYC* activation. Cells were then stained with 5 μmol/L of the fluorescent indicator of oxidative stress, 2′7′-dichlorofluorescein diacetate (DCFDA; Sigma-Aldrich), for 20 minutes, washed with

Note: Supplementary data for this article are available at Cancer Research Online (http://cancerres.aacrjournals.org/).

Requests for reprints: Dean W. Felsher, Department of Medicine, Division of Oncology, Stanford University School of Medicine, 269 Campus Drive, Stanford, CA 94305. Phone: 650-498-5269; Fax: 650-725-1420; E-mail: dfelsher@stanford.edu.

doi:10.1158/0008-5472.CAN-05-3115

PBS, and mounted onto slides using Vetorshield fluorescent mounting medium. Cells treated with 1 μmol/L hydrogen peroxide for 15 minutes were used as a positive control. Fluorescent images of ~100 cells from multiple fields per sample were viewed under a 20× objective using a FITC filter in a Confocal Microscope (Nikon, PCM2000, with a Spot Camera) and quantitated using Metamorph software (Universal Imaging Corp., Downingtown, PA; refs. 32, 33).

Flow cytometry analysis for detecting ROS. For *in vitro* studies, NHF-*MYCER* cells were grown in normal (10%) and low (0.05%) serum in six-well tissue culture dishes and *MYC* was induced for 4 hours with 4-OHT. Cells were treated with antioxidant NAC overnight, before *MYC* activation. Generation of ROS was measured by flow cytometry using DCFDA at a final concentration of 5 μmol/L at 37°C for 20 minutes. Cells untreated with 4-OHT were used as a negative control whereas cells treated with 1 μmol/L hydrogen peroxide for 15 minutes were used as a positive control.

To study if ambient oxygen conditions in the laboratory influenced the production of ROS, NHF-*MYCER* cells grown in normal (10%) or low (0.05%) serum were cultured under different oxygen concentrations (2% and 20%) and ROS was measured by fluorescence-activated cell sorting (FACS) after inducing *MYC* for 4 hours by methods mentioned above.

For *in vivo* studies to determine ROS, we used the transgenic Eμ*MYC*/tTA mice expressing *MYC* conditionally under the influence of the tetracycline activating protein (30). One-month-old mice in which *MYC* was either activated since birth or inactivated using doxycycline were sacrificed and thymocytes were isolated by standard methods. Cells were then stained with DCFDA and assayed for ROS as above. Cells were exogenously treated with 1 μmol/L hydrogen peroxide for 15 minutes to generate DNA breaks. Cohorts of two to four mice were used for each condition per experiment.

Comet assay for detection of DNA breaks. NHF-*MYCER* cells were grown asynchronously in normal (10%) or low (0.05%) serum and treated with or without antioxidant NAC, overnight, before *MYC* induction. *MYC* was induced with 4-OHT and Comet assay for detection of DNA breaks was done with partial modifications of previously published protocols (34). Cells were embedded in low melting agarose on frosted glass slides precoated with two layers of 1% agarose. Cells were lysed in a lysis buffer (2.5% SDS, 2.5 mol/L NaCl, 0.1 mol/L EDTA, pH 10) to detect both DSBs and SSBs/oxidative base changes and electrophoresed for 20 minutes at 25 V and 200-mA current from negative to positive direction. Cells were stained with ethidium bromide, wet-mounted with cover-slips, and observed under an epifluorescence microsope (Nikon). DNA breaks were analyzed in 100 cells per sample and quantified using the HCSA (High Capacity Slide Analyzer) program and KOMET software (LAI, Inc., Laredo, TX). Mean moment of the comets was measured in arbitrary units.

FACS assays for apoptosis. NHF-*MYCER* cells were grown in normal (10%) and low (0.05%) serum in six-well tissue culture dishes and *MYC* was induced for 4 hours with 4-OHT. Staining of the cells with propidium iodide was done according to standard protocols (9). Anti-caspase-3 antibody staining was done using the BD PharMingen caspase-3 staining kit and cells were analyzed by flow cytometry. Cells treated with 5 μmol/L hydrogen peroxide were used as a positive control whereas uninduced cells were used as a negative control. A total of 100 cells were imaged for each sample analyzed.

Double immunofluorescence staining for detection of SSBs and DSBs. For *in vitro* studies to characterize the types of breaks observed on *MYC* induction, NHF-*MYCER* cells were grown in normal and low serum on coverslips in 24-well tissue culture dishes. *MYC*-induced and uninduced cells were fixed with cold methanol and stained with a blend of anti-Ape-1 (Santa Cruz Biotechnology, Santa Cruz, CA) and anti-γH2AX antibodies (Upstate, Charlottesville, VA). FITC-conjugated antirabbit (Sigma-Aldrich) and Alexa Fluor 594–conjugated antimouse (Molecular Probes) secondary antibodies were used against the respective primary antibodies. Cells were mounted in Vector Shield mounting medium containing 4′,6-diamidino-2-phenylindole (DAPI) and viewed under an immunofluorescence microscope (Nikon, Eclipse E800, with FDX-35 camera) with FITC and tetramethylrhodamine isothiocyanate filters to observe staining against Ape-1 and γH2AX antibodies. Nuclear staining was done with DAPI and slides were viewed under a UV filter. Multiple images for each sample were captured and analyzed. Cells irradiated with 2 Gy of γ-radiation from a cesium source and cells treated with 1 μmol/L hydrogen peroxide were used as positive controls for generating DSBs and SSBs, respectively. A total of 100 cells from multiple fields were imaged for each sample analyzed.

For *in vivo* studies to characterize the types of DNA breaks, we used the transgenic Eμ-tTA/tet-o-*MYC* mice described above. One-month-old mice in which *MYC* was activated constitutively were sacrificed and thymocytes were isolated by standard methods. After lysis and removal of RBC with ACK buffer containing 0.15 mol/L ammonium chloride, 1 mmol/L potassium bicarbonate, and 0.1 mmol/L sodium salt of EDTA, thymocytes were spotted on poly-L-lysine–coated coverslips. Cell spots were fixed in cold methanol and immunostaining was done by methods described above. Whereas thymocytes from *MYC*-inactivated mice were used as a negative control, cells irradiated with 2 Gy of γ-radiation from a cesium source and cells treated with 1 μmol/L hydrogen peroxide were used as positive controls for generating DSBs and SSBs, respectively. For each experiment, cohorts of two to four mice were used for per condition and 100 cells were examined from different fields for each sample analyzed.

cDNA microarray. RNA was extracted after 4 hours of *MYC* induction in NHFs grown in normal (10%) or low (0.05%) serum using standard protocols. cDNA microarray was done using slide-based microarrays manufactured at the Stanford Functional Genomics Facility.[4] These arrays contained >40,000 spots representing ~25,800 genes as estimated by Unigene Clusters. About 50 μg of total RNA were used and subsequent hybridizations were carried out according to the Brown Lab protocols.[5] The Stratagene Universal Human Reference RNA representing total RNA pooled from 10 different cell lines was used as reference. The hybridized arrays were scanned and the data extracted using Genepix 3.0 Software (Axon Instruments) and stored at the Stanford Microarray Database for analysis.

To identify genes that were differentially regulated by *MYC* in normal and low serum conditions, we first filtered genes for adequate technical measurements, as judged by hybridization intensities of 1.5-fold over the local background in both Cy5 (experimental) and Cy3 (reference) channels. For each serum condition, we subtracted the log 2 value of the *MYC*-off samples from the *MYC*-on samples; the resulting value indicated the fold change caused by *MYC* induction. We selected genes that had at least a 2-fold change in response to *MYC* in either condition. This subset of genes was organized by hierarchical clustering to group genes based on the similarity in their patterns of regulation by *MYC*.

Real-time quantitative reverse transcription-PCR. RNA was extracted from *MYC*-induced and uninduced NHF-*MYCER* cells grown in normal (10%) or low (0.05%) serum using TRIZOL reagent and following standard RNA extraction protocols. cDNA was synthesized with oligo-dT using Superscript first-strand synthesis system for reverse transcription-PCR (RT-PCR; Invitrogen, Inc., Carlsbad, CA). Relative quantitation of mRNA for the 2C9 isoform of *CYP450* (*CYP2C9*), superoxide dismutase 2 (*SOD2*), and cytochrome *c* oxidase, isoform 7C (*COX7C*) genes was done by real-time quantitative RT-PCR using SYBR Green (Applied Biosystems, Foster City, CA) and the 7900 ABI Prism Instrument. The primers were designed using the PRIMER 3 software and *GAPDH* was used as the housekeeping gene. PCR primers were *CYP2C9*: (sense) 5′-GGGCCTCAGACTACATCCAA-3′, (antisense) 5′-GGCAAAGGTGGAAATGAAGA-3′; *COX7C*: (sense) 5′-GCATTTTAAGAGGTGCAGCC-3′, (antisense) 5′-ATACAGAGTGAACACCGGGC-3′; *SOD2*: (sense) 5′-GGCAAAGGTGGAAATGAAGA-3′, (antisense) 5′-GGGCCTCAGACTACATCCAA-3′; and *GAPDH*: (sense) 5′-TGCACCACCAACTGCTTAGC-3′, (antisense) 5′-GCATGGACTGTGGTCATGAG-3′. The results were analyzed graphically using the ΔΔCt method (35).

Immunoblotting for CYP2C9. Western blot analysis for CYP2C9 isoform was done by standard techniques in *MYC*-induced NHF-*MYCER* cells grown in normal and low serum. Anti-CYP2C9 antibody (Gentest, San Jose, CA) was used as primary antibody whereas antirabbit horseradish

[4] http://genome-www5.stanford.edu/MicroArray/SMD.
[5] http://cmgm.Stanford.EDU/pbrown/.

peroxidase (HRP) conjugate was used as secondary antibody. α-Tubulin (Calbiochem, San Diego, CA) was used as a loading control and anti-mouse HRP conjugate (Amersham Biosciences, Piscataway, NJ) was used as secondary antibody.

RNA interference against *CYP2C9*. Small interfering RNA was obtained commercially from Ambion (Austin, TX) and transiently transfected into uninduced or *MYC*-induced NHFs according to the instructions of the manufacturer using Oligofectamine (Invitrogen). *MYC*-induced cells that were either untransfected or transfected with an unrelated small interfering RNA (*CDK2*) were used as controls.

Inhibition of *CYP2C9* using sulfaphenazole. Sulfaphenazole (Sigma) was added to *MYC*-induced NHF-*MYCER* cells grown in normal and low serum and any change in the generation of ROS was analyzed by FACS as mentioned above.

Statistical analysis. To determine the statistical significance of our results, we calculated *P* values for all our experiments by the standard *t* test method.

Results

MYC induces ROS production in low serum or ambient oxygen saturation. Recent reports suggest that MYC can induce DNA damage through the production of ROS (10, 23, 36). However, these experiments were done in NHFs that had been adapted to growth in 10% serum and ambient supraphysiologic oxygen saturation (20%). We investigated if MYC induced ROS in NHFs growing in physiologic conditions. We found that *MYC* overexpression *in vitro* in NHFs causes significant increase in ROS above background when grown in low serum (0.05%) and ambient oxygen saturation (P = 0.001), as measured by either confocal microscopy (Fig. 1*A* and *B*) or FACS analysis (Fig. 1*C*). Levels of ROS production by *MYC* were comparable to NHFs treated *in vitro* with hydrogen peroxide (Fig. 1*B* and *C*). However, MYC failed to induce significant levels of ROS in NHFs grown in normal serum (10%; P = 0.4638) and/or physiologic oxygen saturation (2%; P = 0.4638; Fig. 1*D*). Notably, MYC also failed to induce ROS in NHFs grown in normal serum but cells were arrested in the cell cycle through contact inhibition, as validated by FACS analysis (data not shown). Hence, MYC induces significant amounts of ROS only in NHFs grown in low serum and ambient oxygen saturation.

MYC can induce DNA breaks through a ROS-independent mechanism. Although *MYC* induced insignificant amount of ROS in NHFs grown in normal serum and physiologic oxygen saturation, *MYC* induction within 4 hours induced DNA breaks in >90% of NHFs irrespective of growth conditions as detected by the Comet assay, modified as previously described to detect both

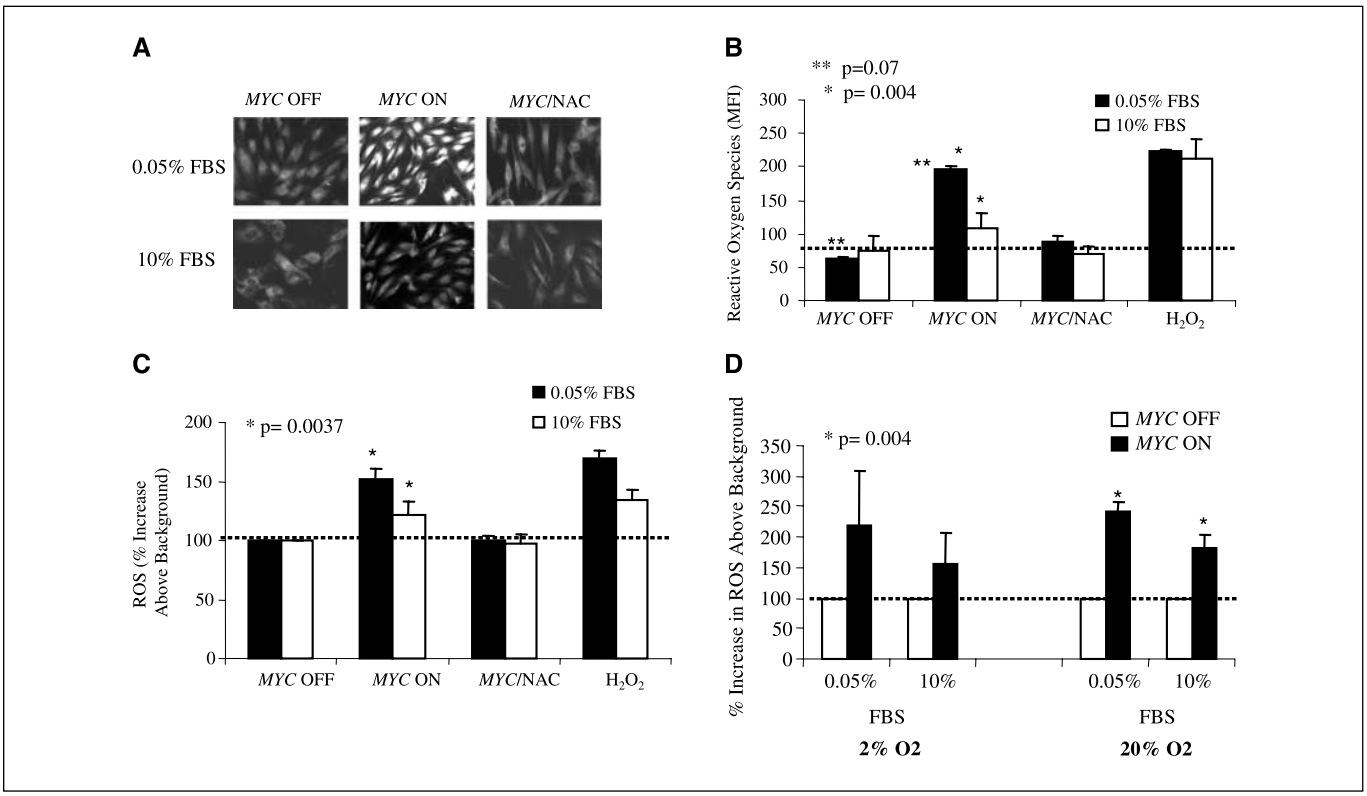

Figure 1. *MYC* induces ROS production in NHFs grown in low serum and nonphysiologic oxygen concentrations. *MYC* was activated for 4 hours with 1 μmol/L 4-OHT in NHF-*MYCER* cells maintained in low (0.05%) or normal (10%) serum in the presence and/or absence of antioxidant NAC. Cells were stained with DCFDA for detection of ROS and viewed by confocal microscopy (*A*) and the fluorescence intensity (*B*) was quantitated using Metamorph software. Statistical significance between MYC-induced ROS production in low versus normal serum was proved by unpaired *t* test that gave a *P* value of 0.004. The amount of ROS generated by MYC in normal serum was statistically insignificant (P = 0.07). *C,* mean fluorescence intensity of DCFDA in *MYC*-induced NHF-*MYCER* cells was measured by flow cytometry. Uninduced cells stained with DCFDA were used as a negative control to detect background levels of ROS produced in these cells. Uninduced cells treated with 1 μmol/L hydrogen peroxide for 15 minutes were used as a positive control. Cells pretreated with NAC were used to detect any decrease in ROS production. Background level of ROS was normalized to 100%. The amount of ROS generated on *MYC* induction in low serum as against normal serum was found to be statistically significant, giving a *P* value of 0.0037. *D,* NHF-*MYCER* cells were subject to ambient (20%) and physiologic (2%) oxygen concentrations using respective oxygen incubators. Cells were either grown in normal or low serum and *MYC* was activated for 4 hours using 4-OHT. Cells were stained with DCFDA and analyzed by flow cytometry for generation of ROS as a measure of mean fluorescence intensity. Representative of three reproducible experiments. *Dotted line,* background level of ROS, normalized to 100%. Statistical significance of *MYC*-induced ROS in low serum and 20% O_2 was proved by unpaired *t* test (P = 0.0037). MYC-induced ROS in normal serum and 2% O_2 was found to be insignificant (P = 0.4638) when compared with background levels of ROS in the cells.

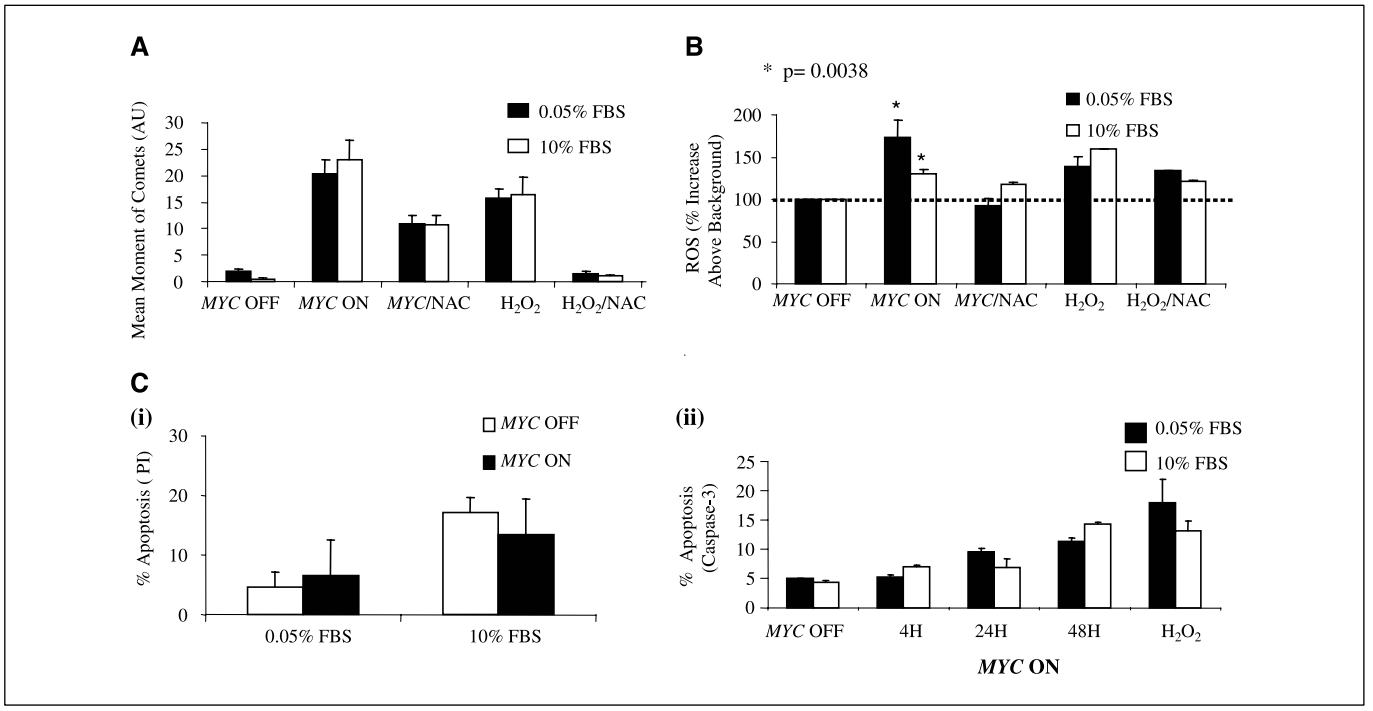

Figure 2. *MYC* induces DNA breaks *in vitro* both dependent and independent of ROS production. *MYC* was activated for 4 hours in NHF-*MYCER* cells grown in low and normal serum. Cells were either subjected to Comet assay (*A*) for detection of DNA breaks or stained with DCFDA and analyzed by flow cytometry (*B*) to investigate ROS production. DNA breaks were quantitated using the HCSA program and the KOMET Software. *A,* for each condition, 100 cells were imaged and mean moment of the comet tails was analyzed in arbitrary units as a measure of DNA breaks. *B,* for detection of ROS, mean fluorescence intensity of DCFDA-stained cells was acquired by FACS and analyzed graphically. For detection of ROS as well as DNA breaks, uninduced cells were used as a negative control and cells treated exogenously with hydrogen peroxide to induce ROS and/or DNA damage were used as a positive control. Cells pretreated with antioxidant NAC were used to detect any change in production of ROS or DNA breaks induced by ROS. *B, dotted line,* background level of ROS. Statistical significance was proved by unpaired *t* test that gave a *P* value of 0.03 when the amount of ROS generated on *MYC* induction in low serum was compared with that in normal serum. *C,* NHFs stained with propidium iodide (*i*) and anti-caspase-3 monoclonal antibody (*ii*) were analyzed by FACS for percentage of apoptotic cells after *MYC* induction in normal and low serum. Cells treated with 5 μmol/L hydrogen peroxide were used as a positive control whereas uninduced cells were used as a negative control.

DSBs and SSBs (Fig. 2*A* and Supplementary Fig. S1; ref. 35). Notably, after *MYC* induction in normal or low serum, >96% of cells exhibited comet moments above background (0-5 units; Supplementary Fig. S1*Bi,ii*). Moreover, treatment with NAC reduced levels of ROS to background (Fig. 2*B*) but failed to prevent MYC from inducing DNA breaks as measured by the Comet assay (Fig. 2*A* and Supplementary Fig. S1). Often NAC failed to eliminate ROS completely because we used a NAC concentration that is well tolerated by normal cells. Treatment with 1 μmol/L hydrogen peroxide for 15 minutes resulted in DNA damage comparable to *MYC* induction by 1 μmol/L tamoxifen for 4 hours. Although the Comet assay generally is considered capable of distinguishing cells with DNA damage from those undergoing apoptosis, we considered that it was possible that the DNA breaks we were detecting by the Comet assay could instead reflect early apoptosis. Although *MYC* is well known to induce apoptosis, in particular, on induction of cells in low serum, this is not generally observed until well after 4 hours of MYC induction. Thus, as expected, we did not observe any change in apoptosis after 4 hours of *MYC* induction as measured through FACS analysis of propidium iodide (Fig. 2*Ci*) or anti-caspase-3 antibody (Fig. 2*Cii*) staining of the cells. We did observe modest levels of baseline apoptosis in cells grown in full serum as often observed in proliferating cells. Therefore, MYC can induce DNA breaks in NHFs *in vitro* through mechanisms both dependent as well as independent of ROS production and this is not associated with any significant apoptosis (10).

***MYC* can induce DSBs and SSBs through ROS-independent mechanisms.** To quantitatively evaluate whether *MYC* is inducing oxidative damage/SSBs and/or DSBs, a double immunofluorescent assay was developed by staining for Ape-1, which measures oxidative base damage and SSBs (26, 37, 38), and by γH2AX phosphorylation staining, which measures DSBs (39–41). *MYC* was found to induce both oxidative base damage/SSBs and DSBs in NHFs *in vitro* as exhibited by combined staining for both Ape-1 and γH2AX (Fig. 3*A*). The frequency of DNA damage generated by oxidative stress, as measured by Ape-1 staining (FITC), was higher (76%) in cells in low serum as compared with cells in normal serum (27%; $P = 0.0025$) and decreased significantly ($P = 0.0024$) on treatment with NAC (25% in low serum and 10% in normal serum; Fig. 3*B* and *C*). In contrast, there was a statistically insignificant difference ($P = 0.4915$) in DSBs (33%) in *MYC*-induced NHFs grown in low serum as compared with normal serum (22%). This frequency did not decrease on treatment with NAC (35% in low serum and 22% in normal serum) as measured by γH2AX staining (Alexa Fluor 594; Fig. 3*B* and *C*). Therefore, *MYC* induces DNA breaks through multiple mechanisms depending on physiologic circumstances: (*a*) oxidative damage/SSBs through ROS production in low serum and (*b*) DSBs independent of ROS production, irrespective of serum concentrations.

Elevated levels of *CYP2C9* correlate with *MYC*-induced ROS in NHFs in low serum. To better characterize the mechanism by which *MYC* induces oxidative damage in low serum, we carried out cDNA microarray analysis of *MYC*-induced NHFs grown in low

versus normal serum (Supplementary Fig. S3). We sought genes that were selectively induced by MYC in low serum and had plausible functions in mediating oxidative stress. Supplementary Table S1 shows a list of genes that are listed in the order presented in Supplementary Fig. S3. "+" indicates increased expression on *MYC* induction whereas "−" indicates decreased expression on *MYC* induction; n.c. indicates no change on *MYC* induction. Indeed, *MYC* regulation of downstream genes was strikingly different in low versus normal serum (Supplementary Fig. S3; Supplementary Table S1). Our results show that cluster "b" included many genes that were repressed by *MYC* in normal serum but induced by *MYC* in low serum. This profile fits our objective criteria defined by other experimental observations. ROS production is mediated through specific isozymes of *CYP450* (29, 42, 43). In particular, the isozyme, *CYP2C9*, has been shown to responsible for ROS in several cell types (44). We noted that *CYP2C9*, a gene with known role in oxidative stress, was up-regulated among genes selectively induced by *MYC* in low serum and was a member of cluster b (Supplementary Fig. S3). Hence, *CYP2C9* was chosen for further study. Other candidate genes, such as the mitochondrial superoxide dismutase (*SOD2*), an antioxidant that has been previously implicated in *MYC* associated ROS production (36), were found to be down-regulated on *MYC* induction, but this occurred irrespective of serum concentration. Thus, *SOD2* is not likely to account for the differences we observed in ROS production in normal versus low serum. Similarly, *COX7C*, an isoform of cytochrome *c* oxidase known to be up-regulated on apoptosis (45), was found to be at least initially down-regulated on *MYC* induction in cells grown in low serum, consistent with the notion that changes in ROS were occurring independent of induction of apoptotic programs (ref. 10; Fig. 2*C*).

We further investigated the potential of *CYP2C9* in mediating ROS production by *MYC*. First by quantitative RT-PCR and second by Western blot analysis, we confirmed that MYC overexpression resulted in a 3-fold increase in *CYP2C9* mRNA (Fig. 4*A*), associated with a 2-fold increase in CYP2C9 protein expression (Fig. 4*B*), in low serum versus normal serum. In addition, we observed a decrease in *SOD2* mRNA levels in *MYC*-induced cells both in low and normal serum whereas *COX7C* expression was repressed in *MYC*-induced cells in low serum (Fig. 4*A*). Next, we directly tested if *CYP2C9* mediates ROS production induced by *MYC*. RNA interference against *CYP2C9* inhibited *MYC*-induced ROS production (Fig. 4*C*). As a positive control, we validated that RNA interference against *CYP2C9* blocked ROS caused by treatment of cells with hydrogen peroxide. *MYC*-activated cells that were either untransfected or transfected with an unrelated control small interfering RNA (*CDK2* in this case) did not show any decrease in ROS, providing evidence of the specificity of the reduction of ROS observed using small interfering RNA against *CYP2C9*.

Treatment with sulfaphenazole (Fig. 4*D*), a specific *CYP2C9* inhibitor, also inhibited *MYC* from inducing ROS. We conclude that *CYP2C9*, at least in part, contributes to ROS production mediated by *MYC* induction in serum-starved cells.

***MYC* induces DSBs *in vivo* independent of ROS.** Finally, we evaluated whether MYC overexpression can induce DSBs *in vivo*. *MYC* was activated in murine lymphocytes using the Tet system as previously described (30). *MYC* was found to induce DNA breaks as detected by the Comet assay (Fig. 5*A* and Supplementary Fig. S5*A*). Although the amount of DNA breaks in hydrogen peroxide–treated uninduced thymocytes was higher compared with *MYC*-activated thymocytes *in vivo*, the pattern of cellular distribution of comet moments in *MYC*-activated thymocytes

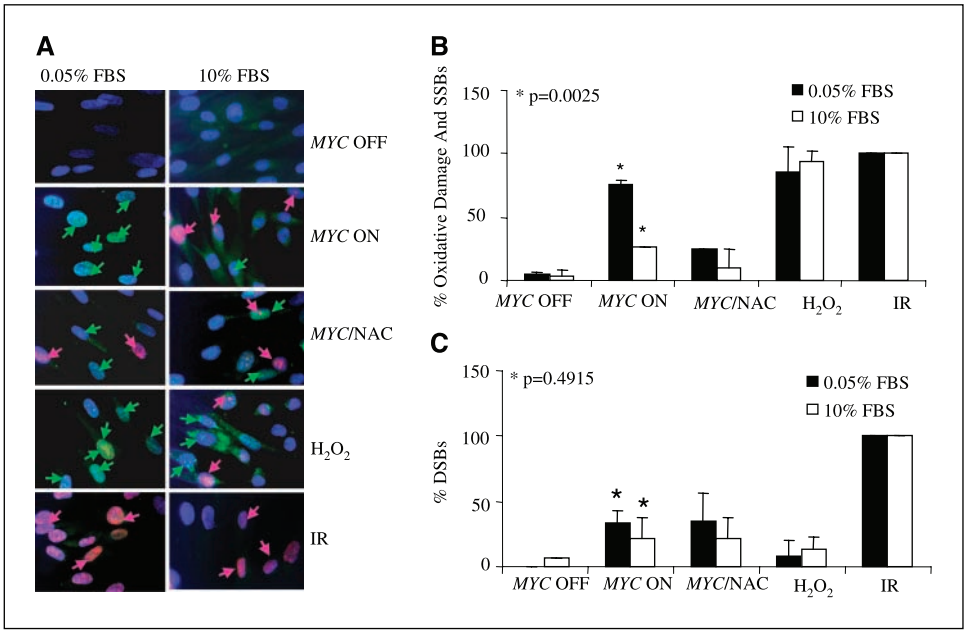

Figure 3. *MYC* induces oxidative damage and DSBs *in vitro*. NHF-*MYCER* cells were grown in low and normal serum and treated with 4-OHT for 4 hours to activate *MYC*. Cells were then fixed in cold methanol and stained with anti-Ape-1 and γH2AX antibodies for detection of SSBs and DSBs, respectively. Cells were incubated with FITC-conjugated antirabbit (*green*) and Alexa Fluor 594–conjugated antimouse (*red*) secondary antibodies against Ape-1 and γH2AX, respectively. Cells were counterstained with DAPI for nuclear staining. *A,* multiple images of cells stained against Ape-1 (base damage/SSBs; *green*) and γH2AX (DSBs; *red*; *arrows*) were visualized and captured using an epifluorescence microscope. Cells were exogenously treated with 1 μmol/L hydrogen peroxide for 15 minutes or subjected to 2 Gy of γ-irradiation to induce DNA breaks and NAC was administered to the cells to function as an antioxidant to reduce DNA damage generated by ROS. *B* and *C,* the amount of oxidative damage/SSBs and DSBs induced due to *MYC* overexpression in different serum conditions was expressed as a percentage of total cells counted. SSBs generated by *MYC* in low serum were statistically significant ($P = 0.0018$) as against uninduced cells or *MYC*-induced cells treated with NAC ($P = 0.0024$). DSBs generated by *MYC* were, however, statistically significant both in low as well as in normal serum ($P < 0.05$, 95% confidence interval).

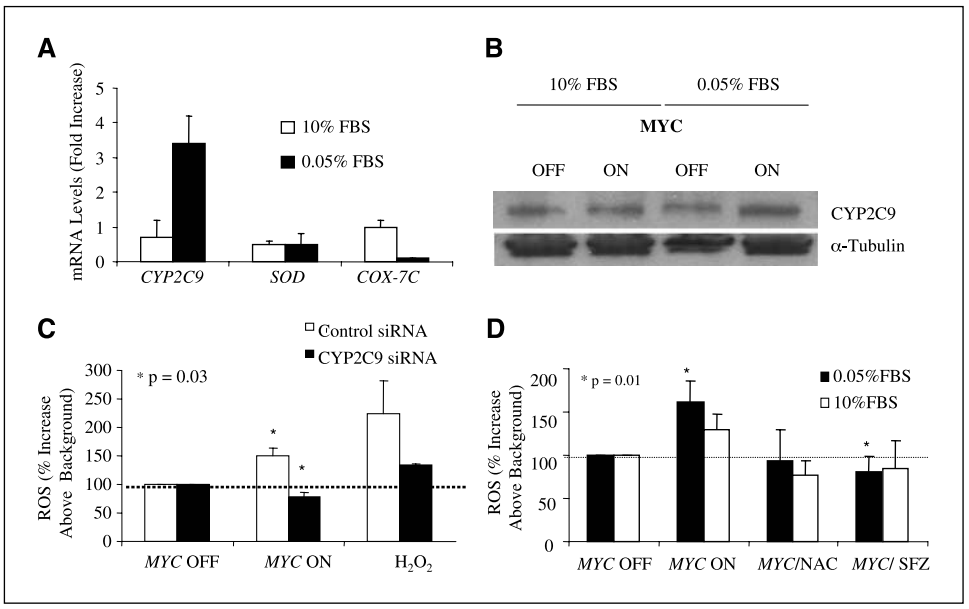

Figure 4. *MYC*-induced ROS in NHFs *in vitro* correlate with *MYC*-induced overexpression of *CYP2C9* in low serum. *A,* fold changes in mRNA expression levels of *CYP2C9, SOD2*, and *COX7C* genes by real-time RT-PCR. *B,* changes in protein levels of CYP2C9 in *MYC*-induced NHF-*MYCER* cells in low and normal serum. *C, MYC* was induced in NHF-*MYCER* cells and mean fluorescence intensity of DCFDA in these cells was measured by flow cytometry. Graphical quantitation for ROS assay in NHF-*MYCER* cells (*A*) transfected with *CYP2C9* small interfering RNA (*B*) treated with 10 μmol sulfaphenazole. Statistical significance was proved by *t* test.

resembled more closely that of cells treated with hydrogen peroxide than that of uninduced thymocytes (Supplementary Fig. S5*B*). Thus, MYC overexpression *in vivo* in lymphocytes can cause DNA damage.

MYC overexpression *in vivo* in murine lymphocytes was not found to induce a measurable increase in ROS production as measured by FACS analysis of DCFDA staining of the cells (P = 0.78; Fig. 5*B*). As a positive control, lymphocytes incubated exogenously with hydrogen peroxide exhibited measurable amount of ROS, in turn associated with DNA breaks detected by Comet assay (Fig. 5*A* and *B*).

Finally, *MYC*-activated thymocytes showed a predominance of γH2AX over inactivated ones, indicative of significant generation of DSBs (60%; P = 0.002) but not SSBs (27%; P = 0.614; Fig. 5*Cii*), proving that *MYC*-induced DSBs are independent of ROS as observed from Ape-1 staining of hydrogen peroxide–treated and γ-irradiated thymocytes from *MYC*-inactivated mice. Notably, similar to our *in vitro* data, *MYC* activation *in vivo* did not induce detectable apoptosis by Annexin V staining (data not shown). Thus, *MYC* induction in lymphocytes *in vivo* can result in DNA breaks independent of ROS and this is not associated with any apoptosis.

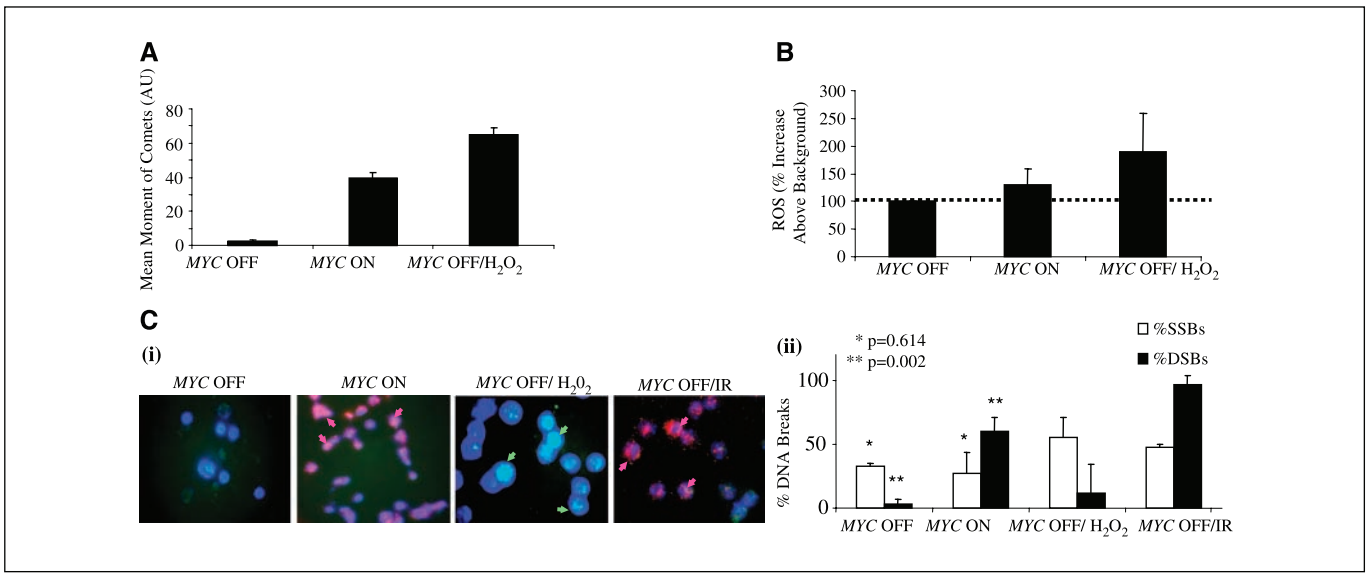

Figure 5. *MYC* induction fails to induce ROS but generates DSBs *in vivo* in murine lymphocytes. *MYC* was either constitutively active or inactivated (with doxycycline) in Eμ-tTA/tet-o-*MYC* mice for 4 weeks since birth. *A,* thymocytes isolated from these mice were subjected to Comet assay for detection of DNA breaks, which were quantified in arbitrary units, as a measure of the mean moment of the comet tails using the KOMET software. *B,* thymocytes from *MYC*-activated or inactivated mice in (*A*) were stained with DCFDA and analyzed by flow cytometry to investigate ROS production. *Dotted line,* background levels of ROS, normalized to 100%. *C, i,* thymocytes from the above mice were fixed in cold methanol and stained as above (Fig. 3) with anti-Ape-1 and γH2AX antibodies for detection of SSBs and DSBs, respectively. Cells exogenously treated with 1 μmol/L hydrogen peroxide for 15 minutes or subjected to 2 Gy of γ-irradiation to induce DNA breaks were used as control. *ii,* the amount of oxidative damage/SSBs and DSBs induced due to *MYC* overexpression in different serum conditions was expressed as a percentage of total cells counted. The amount of DSBs detected in *MYC* activated thymocytes was statistically significant (P = 0.002) when compared with the inactivated thymocytes but that of SSBs was not.

Discussion

MYC overexpression is generally presumed to cause tumorigenesis by inducing unrestrained cellular proliferation and to be restrained from causing tumorigenesis by inducing proliferative arrest, senescence, and/or apoptosis (1, 7, 9, 15). Here we show that MYC overexpression both *in vitro* and *in vivo* induces frequent DNA breaks. Our results are consistent with a multitude of reports that *MYC* can induce genomic instability (3–5, 7–13, 45). One caveat to these studies is that many of these experiments were done *in vitro*. Several reports have suggested that *MYC* induces genomic instability *in vivo* (6, 16, 17). Our results are consistent with these findings. We report that *MYC* overexpression *in vivo* in normal murine lymphocytes can induce DSBs. Notably, DNA breaks were detected to be not associated with increased ROS.

Our results seem to be in discordance with reports that *MYC* induces DNA breaks through ROS (10, 36). To account for this difference, we considered that these experiments had been done at ambient oxygen saturation and/or low serum concentration, both circumstances known to influence ROS production (46, 47). Indeed, *MYC* activation *in vivo* or *in vitro* under physiologic oxygen saturation does not result in the induction of increased ROS production but does result in the formation of DNA breaks. However, *MYC* activation *in vitro* in NHFs cultured in ambient oxygen saturation and/or low serum exhibited increased ROS production, which in turn was associated with the formation of oxidative damage of DNA and SSBs. Most importantly, *MYC*-induced DNA breaks yet failed to induce ROS *in vivo* in normal murine lymphocytes, a cellular subcompartment in which *MYC* activation is frequently associated with tumorigenesis. Thus, *MYC* seems to induce ROS only under specific growth circumstances that do not seem to approximate what is observed *in vivo* in hematopoietic compartments. Hence, *MYC* can cause DNA damage in lymphoid cells even independent of ROS. However, our results are consistent with the possibility that *MYC* can induce ROS under some growth circumstances. Indeed, it has been observed that *MYC* induces ROS production *in vivo* in the liver (6, 48).

We were in part able to account for why *MYC* induced ROS in low serum by showing that MYC induces *CYP2C9*, which has previously been shown to mediate ROS production (44). The inhibition of *CYP2C9* with RNA interference or a small-molecule inhibitor was sufficient to reduce *MYC*-associated ROS production. The mechanism(s) by which MYC induces *CYP2C9*, however, remains to be determined. MYC overexpression also resulted in decreased expression of *SOD2*, consistent with what has recently been described (36). However, *MYC*-induced changes in *SOD2* did not correlate with changes in serum concentration and thus are unlikely to account for the changes in ROS production that we observed. Most likely, *MYC* induces ROS production through effects on multiple gene products depending on cell type and growth conditions. We recognize that an alternative explanation for our results is that in low serum, cells are arrested in the cell cycle, and that under these circumstances *MYC* may induce ROS. Although we cannot rule out this possibility, we did not observe that *MYC* induces ROS in cells that have been arrested in the cell cycle through contact inhibition (data not shown).

Therefore, MYC overexpression results in DNA breaks through different mechanisms depending on growth conditions. MYC overexpression in cells cultured in low serum and/or ambient oxygen results in increased ROS production associated with predominantly SSBs. However, MYC overexpression in cells cultured in normal serum and physiologic oxygen saturation results in frequent DSBs with very modest amount of ROS production. The mechanism by which *MYC* induces DSBs is not clear. *MYC* does not block activation of H2AX; thus, initial recognition of DNA damage is unlikely to be affected. DNA damage, in turn, activates a DNA damage response and results in cell cycle arrest, senescence, or apoptosis (7, 15). MYC could interfere with DNA repair, possibly indirectly, by preventing cell cycle arrest. The loss of p19ARF/p53 function would cooperate with *MYC* to induce tumorigenesis by abrogating some of these checkpoint mechanisms (9, 45, 49). Alternatively, MYC may disrupt formation of DNA repair complexes and/or disrupt chromatin structure, preventing efficient DNA repair. In this regard, it is provocative that loss of H2AX is frequently associated with *MYC* activation, suggesting that they could cooperate to induce tumorigenesis (50).

Our results support the notion that MYC overexpression can induce widespread DNA damage in normal cells *in vitro* and *in vivo* through mechanisms independent of ROS. DNA damage induced by *MYC* could provide a potent signal to induce proliferative arrest, senescence, and/or apoptosis (1, 7, 9, 15).

Acknowledgments

Received 8/31/2005; revised 3/19/2006; accepted 4/20/2006.

Grant support: National Cancer Institute grants RO1-CA89305-01A1, CA89305-0351, CA105102, Leukemia and Lymphoma Society Award, Damon Runyon Lilly Clinical Investigator Award, Burroughs Wellcome Clinical Investigator Award, and Emerald Foundation (D.W. Felsher); SOM Dean's Scholarship (S. Ray); NIH grant AI 566223 (K.R. Atkuri); and National Cancer Institute grant T32 CA09151 (D. Deb-Basu).

The costs of publication of this article were defrayed in part by the payment of page charges. This article must therefore be hereby marked *advertisement* in accordance with 18 U.S.C. Section 1734 solely to indicate this fact.

We thank the members of the Felsher Laboratory for their suggestions; P. Hanawalt's and M. Brown's Labs and for help with Comet assays; D. Tree and J. Axelrod for help with Confocal Microscopy; and A. Giaccia for help with variable oxygen incubators (Stanford University). We apologize to colleagues whose papers we did not cite because of editorial restrictions.

References

1. Pelengaris S, Khan M, Evan G. c-MYC: more than just a matter of life and death. Nat Rev Cancer 2002;2:764–76.
2. Oster SK, Ho CS, Soucie EL, Penn LZ. The myc oncogene: marvelously complex. Adv Cancer Res 2002; 84:81–154.
3. Denko NC, Giaccia AJ, Stringer JR, Stambrook PJ. The human Ha-ras oncogene induces genomic instability in murine fibroblasts within one cell cycle. Proc Natl Acad Sci U S A 1994;91:5124–8.
4. Mai S, Fluri M, Siwarski D, Huppi K. Genomic instability in MycER-activated Rat1A-MycER cells. Chromosome Res 1996;4:365–71.
5. Chernova OB, Chernov MV, Ishizaka Y, Agarwal ML, Stark GR. MYC abrogates p53-mediated cell cycle arrest in *N*-(phosphonacetyl)-L-aspartate-treated cells, permitting CAD gene amplification. Mol Cell Biol 1998; 18:536–45.
6. Factor VM, Kiss A, Woitach JT, Wirth PJ, Thorgeirsson SS. Disruption of redox homeostasis in the transforming growth factor-α/c-myc transgenic mouse model of accelerated hepatocarcinogenesis. J Biol Chem 1998; 273:15846–53.
7. Felsher DW, Bishop JM. Transient excess of MYC activity can elicit genomic instability and tumorigenesis. Proc Natl Acad Sci U S A 1999;96:3940–4.
8. Li Q, Dang CV. c-Myc overexpression uncouples DNA replication from mitosis. Mol Cell Biol 1999;19:5339–51.
9. Felsher DW, Zetterberg A, Zhu J, Tlsty T, Bishop JM. Overexpression of MYC causes p53-dependent G_2 arrest of normal fibroblasts. Proc Natl Acad Sci U S A 2000;97: 10544–8.

10. Vafa O, Wade M, Kern S, et al. c-Myc can induce DNA damage, increase reactive oxygen species, and mitigate p53 function: a mechanism for oncogene-induced genetic instability. Mol Cell 2002;9:1031–44.

11. Fest T, Mougey V, Dalstein V, et al. c-MYC overexpression in Ba/F3 cells simultaneously elicits genomic instability and apoptosis. Oncogene 2002;21:2981–90.

12. Karlsson A, Giuriato S, Tang F, Fung-Weier J, Levan G, Felsher DW. Genomically complex lymphomas undergo sustained tumor regression upon MYC inactivation unless they acquire novel chromosomal translocations. Blood 2003;101:2797–803.

13. Woo RA, Poon RY. Activated oncogenes promote and cooperate with chromosomal instability for neoplastic transformation. Genes Dev 2004;18:1317–30.

14. Rockwood LD, Torrey TA, Kim JS, et al. Genomic instability in mouse Burkitt lymphoma is dominated by illegitimate genetic recombinations, not point mutations. Oncogene 2002;21:7235–40.

15. Grandori C, Wu KJ, Fernandez P, et al. Werner syndrome protein limits MYC-induced cellular senescence. Genes Dev 2003;17:1569–74.

16. Felix K, Polack A, Pretsch W, et al. Moderate hypermutability of a transgenic lacZ reporter gene in Myc-dependent inflammation-induced plasma cell tumors in mice. Cancer Res 2004;64:530–7.

17. Taylor C, Mai S. c-Myc-associated genomic instability of the dihydrofolate reductase locus *in vivo*. Cancer Detect Prev 1998;22:350–6.

18. Karlsson A, Deb-Basu D, Cherry A, Turner S, Ford J, Felsher DW. Defective double-strand DNA break repair and chromosomal translocations by MYC overexpression. Proc Natl Acad Sci U S A 2003;100:9974–9.

19. Khanna KK, Jackson SP. DNA double-strand breaks: signaling, repair and the cancer connection. Nat Genet 2001;27:247–54.

20. Hironaka K, Factor VM, Calvisi DF, Conner EA, Thorgeirsson SS. Dysregulation of DNA repair pathways in a transforming growth factor α/c-myc transgenic mouse model of accelerated hepatocarcinogenesis. Lab Invest 2003;83:643–54.

21. Maciag A, Sithanandam G, Anderson LM. Mutant K-rasV12 increases COX-2, peroxides and DNA damage in lung cells. Carcinogenesis 2004;25:2231–7.

22. Maciag A, Anderson LM. Reactive oxygen species and lung tumorigenesis by mutant K-ras: a working hypothesis. Exp Lung Res 2005;31:83–104.

23. Dang CV, Li F, Lee LA. Could MYC induction of mitochondrial biogenesis be linked to ROS production and genomic instability? Cell Cycle 2005;4:1465–6.

24. Louis SF, Vermolen BJ, Garini Y, et al. c-Myc induces chromosomal rearrangements through telomere and chromosome remodeling in the interphase nucleus. Proc Natl Acad Sci U S A 2005;102:9613–8.

25. Jackson AL, Loeb LA. The contribution of endogenous sources of DNA damage to the multiple mutations in cancer. Mutat Res 2001;477:7–21.

26. Ramana CV, Boldogh I, Izumi T, Mitra S. Activation of apurinic/apyrimidinic endonuclease in human cells by reactive oxygen species and its correlation with their adaptive response to genotoxicity of free radicals. Proc Natl Acad Sci U S A 1998;95:5061–6.

27. Slupphaug G, Kavli B, Krokan HE. The interacting pathways for prevention and repair of oxidative DNA damage. Mutat Res 2003;531:231–51.

28. Bondy SC, Naderi S. Contribution of hepatic cytochrome *P*450 systems to the generation of reactive oxygen species. Biochem Pharmacol 1994;48:155–9.

29. Parke DV. The cytochromes *P*450 and mechanisms of chemical carcinogenesis. Environ Health Perspect 1994;102:852–3.

30. Felsher DW, Bishop JM. Reversible tumorigenesis by MYC in hematopoietic lineages. Mol Cell 1999;4:199–207.

31. Eilers M, Picard D, Yamamoto KR, Bishop JM. Chimaeras of myc oncoprotein and steroid receptors cause hormone-dependent transformation of cells. Nature 1989;340:66–8.

32. O'Mahony R, Basset C, Holton J, Vaira D, Roitt I. Comparison of image analysis software packages in the assessment of adhesion of microorganisms to mucosal epithelium using confocal laser scanning microscopy. J Microbiol Methods 2005;61:105–26.

33. Klimaschewski L, Nindl W, Pimpl M, Waltinger P, Pfaller K. Biolistic transfection and morphological analysis of cultured sympathetic neurons. J Neurosci Methods 2002;113:63–71.

34. Olive PL, Wlodek D, Banath JP. DNA double-strand breaks measured in individual cells subjected to gel electrophoresis. Cancer Res 1991;51:4671–6.

35. Livak KJ, Schmittgen TD. Analysis of relative gene expression data using real-time quantitative PCR and the $2(-\Delta\Delta C(T))$ Method. Methods 2001;25:402–8.

36. Tanaka H, Matsumura I, Ezoe S, et al. E2F1 and c-Myc potentiate apoptosis through inhibition of NF-κB activity that facilitates MnSOD-mediated ROS elimination. Mol Cell 2002;9:1017–29.

37. Izumi T, Hazra TK, Boldogh I, et al. Requirement for human AP endonuclease 1 for repair of 3′-blocking damage at DNA single-strand breaks induced by reactive oxygen species. Carcinogenesis 2000;21:1329–34.

38. Angkeow P, Deshpande SS, Qi B, et al. Redox factor-1: an extra-nuclear role in the regulation of endothelial oxidative stress and apoptosis. Cell Death Differ 2002;9:717–25.

39. Banath JP, Olive PL. Expression of phosphorylated histone H2AX as a surrogate of cell killing by drugs that create DNA double-strand breaks. Cancer Res 2003;63:4347–50.

40. Pilch DR, Sedelnikova OA, Redon C, Celeste A, Nussenzweig A, Bonner WM. Characteristics of γ-H2AX foci at DNA double-strand breaks sites. Biochem Cell Biol 2003;81:123–9.

41. Rothkamm K, Lobrich M. Evidence for a lack of DNA double-strand break repair in human cells exposed to very low X-ray doses. Proc Natl Acad Sci U S A 2003;100:5057–62.

42. Schmidt R, Baumann F, Knupfer H, et al. CYP3A4, CYP2C9 and CYP2B6 expression and ifosfamide turnover in breast cancer tissue microsomes. Br J Cancer 2004;90:911–6.

43. Klaunig JE, Kamendulis LM. The role of oxidative stress in carcinogenesis. Annu Rev Pharmacol Toxicol 2004;44:239–67.

44. Fleming I, Michaelis UR, Bredenkotter D, et al. Endothelium-derived hyperpolarizing factor synthase (cytochrome *P*450 2C9) is a functionally significant source of reactive oxygen species in coronary arteries. Circ Res 2001;88:44–51.

45. Yin XY, Grove L, Datta NS, Long MW, Prochownik EV. C-myc overexpression and p53 loss cooperate to promote genomic instability. Oncogene 1999;18:1177–84.

46. Michelakis ED, Thebaud B, Weir EK, Archer SL. Hypoxic pulmonary vasoconstriction: redox regulation of O(2)-sensitive K(+) channels by a mitochondrial O(2)-sensor in resistance artery smooth muscle cells. J Mol Cell Cardiol 2004;37:1119–36.

47. Waypa GB, Schumacker PT. Hypoxic pulmonary vasoconstriction: redox events in oxygen sensing. J Appl Physiol 2005;98:404–14.

48. Nishigori C, Hattori Y, Toyokuni S. Role of reactive oxygen species in skin carcinogenesis. Antioxid Redox Signal 2004;6:561–70.

49. Sherr CJ. Tumor surveillance via the ARF-p53 pathway. Genes Dev 1998;12:2984–91.

50. Bassing CH, Suh H, Ferguson DO, et al. Histone H2AX: a dosage-dependent suppressor of oncogenic translocations and tumors. Cell 2003;114:359–70.